

CATALYTIC PERFORMANCE OF MULTI- COMPONENT COPPER-BASED CATALYST FOR DIRECT CARBON DIOXIDE HYDROGENATION TO METHANOL

KOH MEI KEE

UNIVERSITI SAINS MALAYSIA

2018

**CATALYTIC PERFORMANCE OF MULTI-COMPONENT COPPER-
BASED CATALYST FOR DIRECT CARBON DIOXIDE
HYDROGENATION TO METHANOL**

by

KOH MEI KEE

**Thesis submitted in fulfillment of the
requirements for the degree of
Doctor of Philosophy**

September 2018

ACKNOWLEDGEMENT

The completion of this thesis is one of my most important accomplishments to date, but, it would not have been possible without help. Throughout my research journey, I have worked with many people whose contributions deserved special mention in my humble acknowledgement. I am thankful to God Almighty for these wonderful souls. God is good all the time.

My sincere appreciation goes to Prof Ir. Dr Abdul Rahman Mohamed, my Advisor, for his excellent guidance at all stages of the research. I have learnt invaluable skills and positive work attitudes from him. Most importantly, he has instilled me with the confidence I need to be successful not only in my career, but also in life. He is truly an inspiring Advisor. I also owe many thanks to Prof. Dr Chai Siang Piao from Monash University for his enthusiasm and constructive comments on my research. Having the chance to learn from his example to solve problem, write and present has been an invaluable experience for me.

I would like to thank all the technical and administrative staffs in the School of Chemical Engineering, especially Ms. Nurul Hidayah, Mrs. Noraswani Muhammad, Mrs. Yusnadia Mohd Yusof, Mrs. Latiffah Abd Latiff, Mrs. Normie Hana A. Rahim, Mrs. Nor Ain Mat Yusof, Mr. Muhd Arif Mat Husin, Mr. Shamsul Hidayat Shaharan and Mr. Mohd Roqib Mohd Rashidi. They have kindly offered their service during my study.

I am also grateful to my colleagues in the laboratory: Dr. Khozema Ahmed Ali, Mr. Wong Yee Jie, Ms. Khoo Choon Gek, Ms. Teh Yong Yi, Ms. Lim Rong-Er and many more that I am not able to mention here. I appreciate the time we spent together to share and discuss about our research. These have broadened and enriched my

knowledge. These talented individuals have made my research journey more enjoyable and exciting.

I am truly in debt to my husband, Mr. Ang Soon Thian, for his unwavering supports and words of kindness when I was self-doubting. He is an excellent father to our daughter, Beatrice. He has been taking good care of Beatrice when I was too occupied with work. Beatrice may be too young to understand now but she has been a great motivation for me to complete this work. To my dearest Father, Mr. Koh Poh Chye, thank you for always believing in me. To my beloved Mother, Mrs. Cheong Ngan, thank you for watching over me always. To the rest of my family members, I appreciate their support and encouragement.

Last but not least, I am grateful to the Ministry of Education Malaysia for funding the research via long-term research grant scheme Universiti Sains Malaysia-NanoMITE (203/PJKIMIA/6720009) and my scholarship via MyPhd program.

Thank you to All!

Koh Mei Kee
2018

TABLE OF CONTENTS

	Page
ACKNOWLEDGEMENT	ii
TABLE OF CONTENTS	iv
LIST OF TABLES	vii
LIST OF FIGURES	ix
LIST OF ABBREVIATIONS	xiii
LIST OF SYMBOLS	xiv
ABSTRAK	xv
ABSTRACT	xvii
CHAPTER ONE - INTRODUCTION	
1.1 Global methanol demand	1
1.2 Direct carbon dioxide (CO ₂) hydrogenation to methanol	5
1.3 Problem statement	7
1.4 Research objectives	10
1.5 Scope of study	10
1.6 Thesis organization	12
CHAPTER TWO - LITERATURE REVIEW	
2.1 Conversion routes for direct CO ₂ hydrogenation to methanol	14
2.2 Thermodynamic analysis	17
2.3 Reaction mechanisms	20
2.4 Activation of CO ₂ molecules	24
2.5 Heterogenous catalysts for CO ₂ hydrogenation to methanol	27
2.5.1 Copper-based catalysts	28
2.5.2 Palladium-based catalysts	48
2.5.3 Other catalysts	51
2.6 Steps in a catalytic reaction	55
2.7 Summary	57
CHAPTER THREE – MATERIALS AND METHODS	
3.1 Materials and chemicals	59
3.2 Research summary	59

3.3	Experimental setup	63
3.4	Multi-component copper-based catalyst development	64
3.5	Synthesis of siliceous porous supports	66
3.6	Effective diffusivity analysis	67
3.7	Process study	68
3.8	Catalyst stability	69
3.9	Catalyst characterizations	69
3.9.1	Metal content	69
3.9.2	Porous networks and textural properties	70
3.9.3	Structural information at nanometer-scale	70
3.9.4	Surface morphology	71
3.9.5	Elemental mapping	71
3.9.6	Surface crystalline phase	71
3.9.7	Catalyst reducibility	72
3.9.8	Hydrogen adsorption behaviour	72
3.9.9	Carbon dioxide adsorption behaviour	73
3.9.10	Surface chemical states	73
3.9.11	Catalyst performance study	74

CHAPTER FOUR - RESULTS AND DISCUSSION

4.1	Development of multi-component copper-based catalysts	76
4.1.1	Mole ratio of Cu:Zn in SBA-15 supported catalyst	76
4.1.2	Catalyst screening with different promoter	82
4.1.3	Effects of Mn-loading on the performance of Mn-CZ/SBA-15	91
4.1.4	Extensive investigation on the multi-functionality of Mn-CZ/SBA-15	97
4.1.4(a)	Physiochemical properties of catalysts	98
4.1.4(b)	Reduction behaviour of catalysts	107
4.1.4(c)	Adsorption behaviour of catalysts	109
4.1.4(d)	Catalytic performance of catalysts	114
4.2	Morphological impact of porous supports on copper crystallites and effective diffusivity of catalysts	118
4.2.1	Physiochemical properties of porous supports and catalysts	118

4.2.2	Effective diffusivity analysis	127
4.2.3	Catalytic performance of catalysts	128
4.3	Effect of process conditions on catalyst performance	131
4.3.1	Effect of WHSV	131
4.3.2	Effect of reaction temperature	133
4.3.3	Effect of reaction pressure	139
4.4	Catalyst stability	140

CHAPTER FIVE - CONCLUSIONS AND RECOMMENDATIONS

5.1	Conclusions	146
5.2	Recommendations	148

REFERENCES	150
-------------------	-----

APPENDICES

LIST OF PUBLICATIONS

LIST OF TABLES

		Page
Table 2.1	Enthalpy and Gibbs free energy change of methanol synthesis via CO ₂ hydrogenation and RWGS (Centi and Perathoner, 2009; Akarmazyan, 2015).	18
Table 2.2	Summary of past researches on CO ₂ hydrogenation to methanol over heterogenous catalysts.	29
Table 3.1	List of chemicals and reagents.	60
Table 3.2	Details of experiments in process study.	68
Table 4.1	Textural properties of SBA-15 and selected catalysts.	79
Table 4.2	CO ₂ conversion, product selectivity and methanol production rate (Reaction conditions: temperature= 180°C, pressure= 4.0 MPa, WHSV= 60 L/g _{cat} .h, H ₂ :CO ₂ = 3:1 (mole ratio)).	81
Table 4.3	Textural properties and copper crystallite size of catalysts.	85
Table 4.4	CO ₂ conversion, product selectivity and methanol production rate (Reaction conditions: temperature= 180°C, pressure= 4.0 MPa, WHSV= 60 L/g _{cat} .h, H ₂ :CO ₂ = 3:1 (mole ratio)).	89
Table 4.5	Textural properties and copper crystallite size of catalysts with varying Mn-loadings.	93
Table 4.6	Peak maximum temperature, relative peak contribution in H ₂ -TPR profiles and H ₂ /Cu mole ratio.	95
Table 4.7	CO ₂ conversion, product selectivity and methanol production rate (Reaction conditions: temperature= 180°C, pressure= 4.0 MPa, WHSV= 60 L/g _{cat} .h, H ₂ :CO ₂ = 3:1 (mole ratio)).	97
Table 4.8	Notations and weight composition of metal oxide(s) of catalysts.	98
Table 4.9	Textural properties and copper crystallite size of catalysts.	100
Table 4.10	Peak maximum temperature, relative peak contribution in H ₂ -TPR profiles and H ₂ /Cu mole ratio.	108

Table 4.11	Peak maximum desorption temperature and quantitative data of H ₂ -TPD and CO ₂ -TPD.	111
Table 4.12	CO ₂ conversion, product selectivity and methanol production rate (Reaction conditions: temperature= 180°C, pressure= 4.0 MPa, WHSV= 60 L/g _{cat} .h, H ₂ :CO ₂ = 3:1 (mole ratio)).	115
Table 4.13	Notations and weight composition of metal oxide(s) of catalysts.	118
Table 4.14	Textural properties of pure supports and catalysts.	121
Table 4.15	Copper crystallite size and copper surface area after hydrogen reduction and after reaction.	123
Table 4.16	Peak maximum temperature, relative peak contribution in H ₂ -TPR profiles, H ₂ /Cu mole ratio and effective diffusivities of CO ₂ molecules.	126
Table 4.17	CO ₂ conversion, product selectivity and methanol production rate (Reaction conditions: temperature= 180°C, pressure= 4.0 MPa, WHSV= 60 L/g _{cat} .h, H ₂ :CO ₂ = 3:1 (mole ratio)).	129
Table 4.18	Average copper crystallite size and copper surface area of CZM/KIT-6 used in the experiments conducted at 180°C, 220°C and 260°C (other reaction conditions: pressure= 4.0 MPa, WHSV= 60 L/g _{cat} .h, H ₂ :CO ₂ = 3:1 (mole ratio)).	134
Table 4.19	Comparison of apparent activation energies (<i>E_a</i>) of methanol and CO formation attained in current study and in literature.	139
Table 4.20	Average copper crystallite size and copper surface area of pre-reduced CZM/KIT-6 and CZM/KIT-6 spent in the stability experiment (after 120 h time-on-stream).	143
Table 4.21	Comparison of the performance of CZM/KIT-6 and other catalysts reported in literature during stability experiment.	144

LIST OF FIGURES

		Page
Figure 1.1	Global methanol demand by region (Alvarado, 2016).	1
Figure 1.2	Major applications of methanol.	2
Figure 2.1	Reaction mechanism networks of CO ₂ hydrogenation to methanol (Grabow and Mavrikakis, 2011; Zhao <i>et al.</i> , 2011; Tao <i>et al.</i> , 2013; Yang <i>et al.</i> , 2013).	21
Figure 2.2	Coordination modes of CO ₂ molecule to active metal site (Ge, 2013; Liu <i>et al.</i> , 2013).	24
Figure 2.3	XPS data of (a) Zn 2p _{3/2} , (b) O 1s of plate and rod ZnO nanoparticles, (c) O 1s of plate ZnO and its mixture with copper and (d) Cu 2p _{3/2} of metallic copper and its mixture with plate ZnO (Liao <i>et al.</i> , 2011).	36
Figure 2.4	TEM micrographs of reduced Cu/ZnO catalyst at Cu:Zn ratio of 70:30 (Behrens, 2009).	37
Figure 2.5	(a) Cu(111), Cu(211) and CuZn(211) facets considered in DFT calculations and (b) comparison of Gibbs free energy of reaction intermediates calculated for the respective facets (assuming T =500 K and P of 40 bar of H ₂ , 10 bar of CO and 10 bar of CO ₂ , respectively, and 1 bar of methanol and H ₂ O, corresponding to low conversion composition) (Behrens <i>et al.</i> , 2012).	38
Figure 2.6	TOF of methanol vs (a) metallic copper surface area and (b) relative amount of <i>m</i> -ZrO ₂ (Guo <i>et al.</i> , 2010).	44
Figure 2.7	Methanol formation rate as a function of (a) <i>t</i> -ZrO ₂ content and (b) concentration of acidic sites (at 533K) (Samson <i>et al.</i> , 2014).	45
Figure 2.8	TEM micrographs (a, c) and particle size distributions (b, d) of Pd-Cu/SiO ₂ (a, b) and Pd-Cu/SBA-15 (c, d) (Jiang <i>et al.</i> , 2015).	47
Figure 2.9	TEM micrographs and particle size distributions of (a) Cu@m-SiO ₂ and (b) Cu/ZnO@m-SiO ₂ (Yang <i>et al.</i> , 2016).	48
Figure 2.10	(a) Evidence of formate formation by <i>in-situ</i> FTIR ($\nu_{as}(\text{COO})= 1592 \text{ cm}^{-1}$) in temperature-programmed reaction experiments and (b) the corresponding infrared	49

spectra of the formate species at the temperature of their highest superficial concentration (Collins *et al.*, 2005).

Figure 2.11	Structures of perovskite oxides (a) ABO_3 and (b) A_2BO_4 (Li <i>et al.</i> , 2017).	51
Figure 2.12	H_2 -TPD (a) and CO_2 -TPD (b) profiles of perovskite $\text{LaCr}_{0.5}\text{Cu}_{0.5}\text{O}_3$, Cu/LaCrO_3 and LaCrO_3 (Jia <i>et al.</i> , 2009).	52
Figure 3.1	Research summary.	62
Figure 3.2	Schematic diagram of experimental set-up.	63
Figure 4.1	SEM (a, b) and TEM (c, d) micrographs of SBA-15 (a, c) and (4)Cu/ZnO/SBA-15 (b, d).	77
Figure 4.2	N_2 adsorption-desorption isotherms of (a) (4)Cu/ZnO, (b) (1)Cu/ZnO/SBA-15, (c) (4)Cu/ZnO/SBA-15, (d) (7)Cu/ZnO/SBA-15 and (e) pure SBA-15.	78
Figure 4.3	XRD diffraction patterns of (a) (4)Cu/ZnO, (b) (1)Cu/ZnO/SBA-15, (c) (4)Cu/ZnO/SBA-15 and (d) (7)Cu/ZnO/SBA-15.	80
Figure 4.4	N_2 adsorption-desorption isotherms (a) and pore-size distributions (b) of (i) Cr-CZ/SBA-15, (ii) Mn-CZ/SBA-15, (iii) Fe-CZ/SBA-15, (iv) Co-CZ/SBA-15, (v) Ni-CZ/SBA-15 and (vi) CZ/SBA-15.	84
Figure 4.5	XRD diffraction patterns of (a) Cr-CZ/SBA-15, (b) Mn-CZ/SBA-15, (c) Fe-CZ/SBA-15, (d) Co-CZ/SBA-15, (e) Ni-CZ/SBA-15 and (f) CZ/SBA-15.	85
Figure 4.6	H_2 -TPR profiles of (a) Cr-CZ/SBA-15, (b) Mn-CZ/SBA-15, (c) Fe-CZ/SBA-15, (d) Co-CZ/SBA-15, (e) Ni-CZ/SBA-15 and (f) CZ/SBA-15.	87
Figure 4.7	N_2 adsorption-desorption isotherms (a) and pore-size distributions (b) of (i) (0.01)-CZM/SBA-15, (ii) (0.05)-CZM/SBA-15, (iii) (0.09)-CZM/SBA-15.	92
Figure 4.8	XRD diffraction patterns of (a) (0.01)-CZM/SBA-15, (b) (0.05)-CZM/SBA-15 and (c) (0.09)-CZM/SBA-15.	93
Figure 4.9	H_2 -TPR profiles of (a) (0.01)-CZM/SBA-15, (b) (0.05)-CZM/SBA-15 and (c) (0.09)-CZM/SBA-15.	95
Figure 4.10	N_2 adsorption-desorption isotherms (a) and pore-size distributions (b) of (i) C/SBA15, (ii) CZ, (iii) CM, (iv)	99

CZ/SBA15, (v) CM/SBA15, (vi) CZM/SBA15 and (vii) SBA-15.

Figure 4.11	TEM micrographs of (a) C/SBA-15, (b) CZ, (c) CM, (d) CZ/SBA-15, (e) CM/SBA-15 and (f) CZM/SBA-15.	101
Figure 4.12	STEM micrograph of CZM/SBA-15 and the corresponding elemental mapping.	102
Figure 4.13	XRD patterns of pre-reduced (a) C/SBA-15, (b) CZ, (c) CM, (d) CZ/SBA-15, (e) CM/SBA-15 and (f) CZM/SBA-15.	103
Figure 4.14	Cu 2p (a), Cu LMM Auger (b), Mn 2p (c), Zn 2p (d) and Zn LMM Auger (e) XPS spectra of pre-reduced (i) C/SBA15, (ii) CM, (iii) CM/SBA15 and (iv) CZM/SBA15.	105
Figure 4.15	H ₂ -TPR profiles of (a) C/SBA15, (b) CZ, (c) CM, (d) CZ/SBA-15, (e) CM/SBA-15 and (f) CZM/SBA-15.	107
Figure 4.16	H ₂ -TPD profiles of pre-reduced (a) C/SBA-15, (b) CZ, (c) CM, (d) CZ/SBA-15, (e) CM/SBA-15 and (f) CZM/SBA-15.	110
Figure 4.17	CO ₂ -TPD profiles of pre-reduced (a) C/SBA-15, (b) CZ, (c) CM, (d) CZ/SBA-15, (e) CM/SBA-15 and (f) CZM/SBA-15.	113
Figure 4.18	Schematic illustration of CO ₂ hydrogenation to methanol over pre-reduced surface of CZM/SBA15 ('M' represents metal oxide).	116
Figure 4.19	TEM micrographs of (a) SBA-15, (b) CZM/SBA-15, (c) MCF, (d) CZM/MCF, (e) KIT-6 and (f) CZM/KIT-6.	119
Figure 4.20	N ₂ adsorption-desorption isotherms of (a) pure supports and (b) catalysts.	120
Figure 4.21	XRD diffraction patterns of (a) pre-reduced catalysts and (b) spent catalysts of (i) CZM/SBA-15, (ii) CZM/MCF and (iii) CZM/KIT-6.	122
Figure 4.22	H ₂ -TPR profiles of (a) CZM/SBA-15, (b) CZM/MCF and (c) CZM/KIT-6.	125
Figure 4.23	Effect of WHSV on the performance of CZM/KIT-6 at constant reaction temperature (180°C) and pressure (4.0 MPa).	132

Figure 4.24	Effect of reaction temperature on the performance of CZM/KIT-6 at constant WHSV (60 L/g _{cat} .h) and reaction pressure (4.0 MPa).	133
Figure 4.25	Arrhenius plot for methanol formation in (a) overall temperature range and (b) according to high- and low-temperature range.	136
Figure 4.26	Methanol and CO production rate at reaction temperature of 160-260°C.	137
Figure 4.27	Arrhenius plot for CO formation.	138
Figure 4.28	Effect of reaction pressure on the performance of CZM/KIT-6 at constant WHSV (60 L/g _{cat} .h) and reaction temperature (220°C).	140
Figure 4.29	CO ₂ conversion (C_{CO_2}), product selectivity (S_i) and methanol yield (Y_{CH_3OH}) of CZM/KIT-6 in 120 h time-on-stream (Reaction conditions: temperature = 200°C, WHSV = 30 L/g _{cat} .h, H ₂ :CO ₂ mole ratio = 3:1, pressure = 5.0 MPa).	141
Figure 4.30	XRD diffraction patterns of (a) pre-reduced CZM/KIT-6 and (b) CZM/KIT-6 spent in stability experiment (after 120 h time-on-stream).	142

LIST OF ABBREVIATIONS

Abbreviation	Description
BET	Brunauer-Emmett-Teller
BE	Binding energy
CO ₂ -TPD	Carbon dioxide-temperature programmed desorption
FWHM	Full width at half maximum
GC-TCD	Gas chromatography-thermal conductivity detector
H ₂ -TPD	Hydrogen-temperature programmed desorption
H ₂ -TPR	Hydrogen-temperature programmed reduction
IUPAC	International Union of Pure and Applied Chemistry
KIT	Korea Advanced Institute of Science and Technology
MCF	Mesocellulose foam
MSU	Michigan State University
MTO	Methanol-to-olefins
PSD	Pore-size distributions
PtMEOH	Power-to-methanol
RES	Renewable energy sources
RWGS	Reverse water-gas shift reaction
SBA	Santa Barbara Amorphous
SEM	Scanning electron microscopy
TOF	Turnover frequency
TEM	Transmission electron microscopy
WGS	Water-gas shift reaction
WHSV	Weight-hourly space velocity
XRD	X-ray diffraction
XPS	X-ray photoelectron spectroscopy

LIST OF SYMBOLS

Symbol	Description	Unit
T	Temperature	°C or K
P	Pressure	MPa or atm
C_{CO_2}	CO ₂ conversion	%
S_i	Selectivity	%
Y_{CH_3OH}	Methanol yield	%
D_{eff}	Effective diffusivity coefficient	cm ² /s
$D_{K,eff}$	Effective Knudsen diffusivity coefficient	cm ² /s
$D_{12,eff}$	Effective bulk diffusivity coefficient	cm ² /s
θ	Catalyst porosity	cm ³ _{pores} /cm ³ _{catalyst}
τ_m	Tortuosity factor	-
S_g	Total surface area per unit mass	cm ² /g
P_p	Catalyst density	g/cm ³
M_i	Molecular weight	g/mol
D_{12}	Diffusion coefficient for binary gas system	-
σ_{12}	Effective collision diameter	Å
Ω_D	Collision integral	-
D	Copper crystallite size	nm
k	Shape factor	-
λ	X-ray wavelength	nm
β	Full width at half maximum	radian
θ	Diffraction angle	degree
S_{Cu}	Copper surface area per unit mass of catalyst	m ² /g _{cat.}
X_{Cu}	Copper mass fraction	-
d_{Cu}	Average copper crystallite size	nm
h	Time	hour

**PRESTASI PEMANGKIN MULTI-KOMPONEN BERASASKAN TEMBAGA
UNTUK PENGHIDROGENAN LANGSUNG KARBON DIOKSIDA
KEPADA METANOL**

ABSTRAK

Penghasilan metanol melalui penghidrogenan langsung karbon dioksida (CO_2) adalah strategi yang penting untuk mempertingkatkan penggunaan CO_2 dan pendekatan yang praktikal untuk menjamin pembangunan mampan. Pengsintesisan mangkin yang aktif adalah kritikal bagi meningkatkan kecekapan tindak balas ini dan menggalakkan perkembangan teknologi tersebut. Selepas saringan yang rapi, mangkin multi-komponen $0.6\text{Cu}/0.15\text{ZnO}/0.05\text{MnO}/1.0\text{SBA-15}$ (CZM/SBA-15) berjaya dihasilkan. Penggunaan SBA-15 sebagai penyokong mangkin memberi kesan yang menggalakkan pada tekstur mangkin. Penambahan MnO mempertingkatkan saling tindak antara oksida tembaga dan oksida-oksida lain dalam mangkin. Selain itu, MnO juga menggalakkan pembentukan kristal tembaga yang kecil. Dengan demikian, kapasiti penjerapan hidrogen mangkin dipertingkatkan dan menyebabkan kekuatan hidrogenasi mangkin bertambah. Saling tindak yang sederhana antara CZM/SBA-15 dan molekul-molekul CO_2 didapati penting untuk meningkatkan penukaran CO_2 . Kememilihan metanol telah meningkat kepada lebih dari 90% kerana wujudnya kawasan antara muka logam-oksida untuk menstabilkan perantaraan tindak balas. Kemudian, kesan morfologi penyokong berliang pada kristal tembaga dan kemeresapan berkesan (pekali bersandar pada geometri liang) mangkin dikaji. Penyokong silika berliang yang dipilih untuk kajian adalah SBA-15, MCF dan KIT-6. Mangkin yang disokong pada KIT-6 (CZM/KIT-6) didapati mempunyai sifat yang

unggul di kalangan mangkin tersebut. Morfologi KIT-6 membendung palam mesopore dan mempromosikan pembentukan kristal tembaga yang kecil. CZM/KIT-6 juga mampu membendung pertumbuhan kristal tembaga dan kehilangan kawasan permukaan tembaga semasa tindak balas akibat daripada penyekatan liang KIT-6 dan jarak antara kristal tembaga yang lebih besar. Kemerresapan berkesan CZM/KIT-6 yang lebih tinggi membolehkan pemindahan molekul bahan tindak balas ke tapak aktif serta pengalihan produk tindak balas yang lebih berkesan. Seterusnya, kesan halaju ruang berat setiap jam (WHSV, 8-120 L/g_{mangkin} jam), suhu tindak balas (160-260°C) dan tekanan (1.0-5.0 MPa) terhadap prestasi CZM/KIT-6 dikaji. Sambutan penukaran CO₂ dan kememilihan methanol terhadap parameter proses tersebut mematuhi termodinamik tindak balas. Dalam kajian kestabilan, prestasi CZM/KIT-6 sepanjang 120 jam didapati senggara pada tahap yang tinggi. Berbanding dengan mangkin terturun, pertumbuhan kristal tembaga CZM/KIT-6 yang digunakan dalam ujikaji kestabilan adalah 50.7% dan kehilangan kawasan permukaan tembaga adalah 33.9%. Secara purata, penukaran CO₂ mencapai 27.6% dan kememilihan metanol adalah 88.3%. Purata penghasilan metanol adalah 24.4% dan ini sepadan dengan kadar penghasilan metanol sebanyak 71.6 mol/kg_{mangkin} jam.

CATALYTIC PERFORMANCE OF MULTI-COMPONENT COPPER-BASED CATALYST FOR DIRECT CARBON DIOXIDE HYDROGENATION TO METHANOL

ABSTRACT

Methanol production from direct CO₂ hydrogenation is a useful strategy to utilize CO₂ and a practical approach to sustainable development. Improving the efficiency of the reaction is crucial for encouraging the decentralize of the technology and this is achievable via the development of active catalysts. After rigorous screenings, multi-component 0.6Cu/0.15ZnO/0.05MnO/1.0SBA-15 (CZM/SBA-15) was developed in this study. The introduction of SBA-15 as catalyst support effectively improved the catalyst texture. The addition of MnO as promoter created strong interactions between CuO and other oxide species in the catalyst. Besides, MnO also promoted the formation of small copper crystallites. In this way, the hydrogen adsorption capacity of the catalyst was enhanced, leading to strong hydrogenation strength. A moderate interaction between CZM/SBA-15 and CO₂ molecules was found crucial for enhancing CO₂ conversion. The methanol selectivity was remarkably increased to more than 90% due to the availability of metal-oxide(s) interfacial area to stabilize reaction intermediates. Then, the morphological impact of porous supports on copper crystallites and effective diffusivity (catalyst pore-geometry dependent coefficient) of catalyst were investigated. The porous supports selected for investigation were SBA-15, MCF and KIT-6. Among all, KIT-6 supported catalyst (CZM/KIT-6) presented the most superior properties. The morphology of KIT-6 deterred mesopore plugging and favoured the formation of small copper crystallites.

CZM/KIT-6 also possessed greater resistance to copper crystallite growth and loss of copper surface area during reaction due to the pore-confining effect of the porous support and the larger inter-crystallite spacing between copper crystallites. The high effective diffusivity of CZM/KIT-6 enhanced the transfer of reactant molecules to active sites and the removal of reaction products. Next, the effect of weight-hourly space velocity (WHSV, 8-120 L/g_{cat}.h), reaction temperature (160-260°C) and pressure (1.0-5.0 MPa) on the performance of CZM/KIT-6 were investigated. The response of CO₂ conversion and methanol selectivity to these parameters strictly obey the reaction thermodynamic. In stability study, the performance of CZM/KIT-6 during 120 h time-on-stream was maintained at high level. Compared to the pre-reduced catalyst, the copper crystallite growth of CZM/KIT-6 spent in the stability experiment was 50.7% and the loss of copper surface area was 33.9%. On the average, the CO₂ conversion attained was 27.6% and the methanol selectivity was 88.3%. The average methanol yield was 24.4% and this corresponds to methanol formation rate of 71.6 mol/kg_{cat}.h.

CHAPTER ONE

INTRODUCTION

This chapter provides an overall introduction to the research undertaken. The importance of methanol as a global commodity is outlined at the beginning of the chapter, followed by an introduction to the current industrial practice to produce methanol. Next, the potential of producing methanol from direct carbon dioxide (CO₂) hydrogenation is discussed. Finally, the problem statement, research objectives, scope of the study and organization of the thesis are presented.

1.1 Global methanol demand

Methanol is a global commodity with active production in Asia, North and South America, Europe, Africa and the Middle East. The worldwide combined production capacity of methanol (over 90 plants) is amounted to about 110 million metric tons per year (Methanol Institute, 2017). Figure 1.1 illustrates the global methanol demand by region.

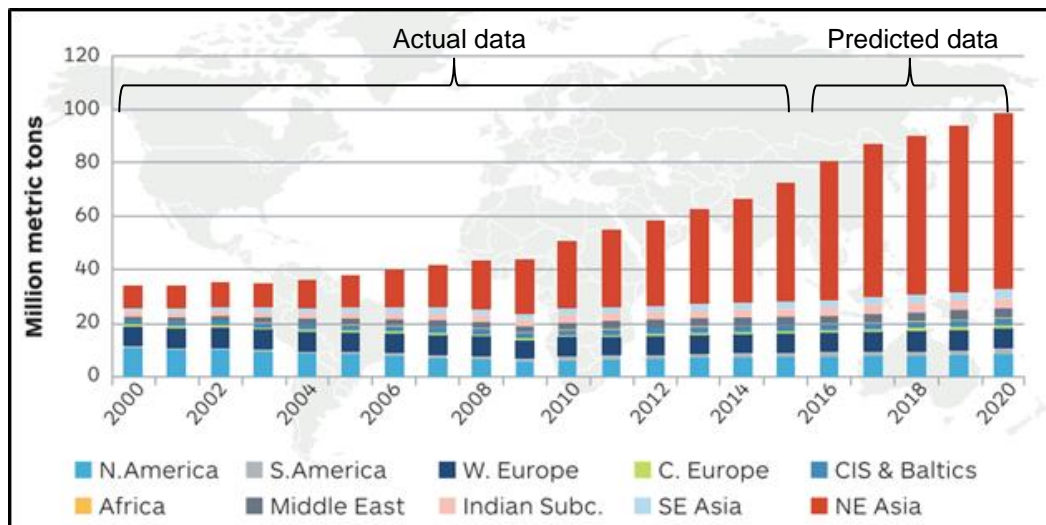


Figure 1.1 Global methanol demand by region (Alvarado, 2016).

The global methanol demand has shown dramatic increases since year 2010 due to the escalating demand in North East Asia. The global demand for methanol has also been predicted to rise above 95 million metric tons by year 2020 and 2021 (Alvarado, 2016; IHS Markit, 2017). In 2015, the global methanol demand had reached 70 million metric tons, mostly due to the growing of energy applications which now account for 40% of the methanol consumption (Methanol Institute, 2017). Each day, nearly 200,000 tons of methanol is used as a chemical feedstock or as a transportation fuel (Methanol Institute, 2017). These statistics confirm that methanol has important role in thriving the global economy now and future.

The high and growing demand for methanol are owed to the fact that methanol has a wide array of applications in our daily lives. Some major applications of methanol are shown in Figure 1.2.

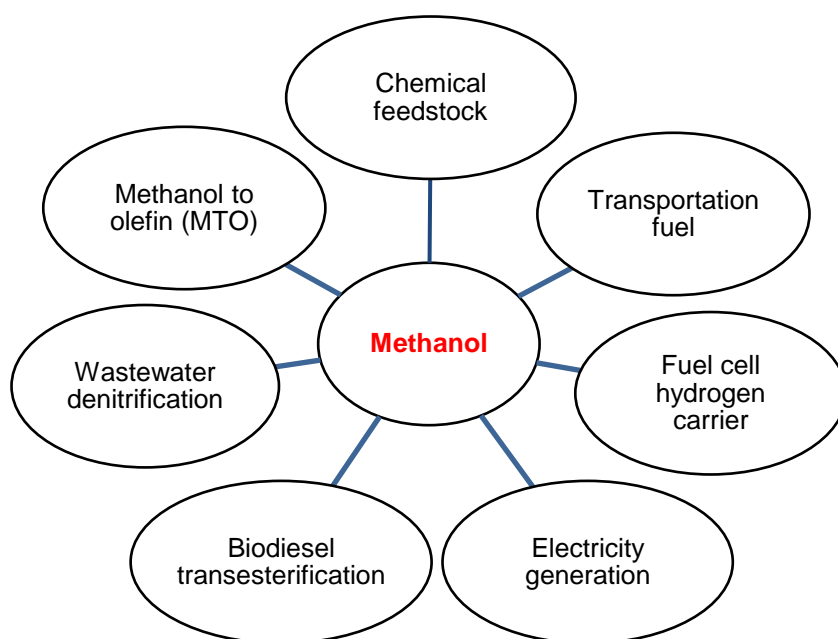
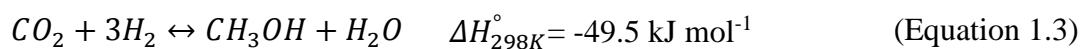
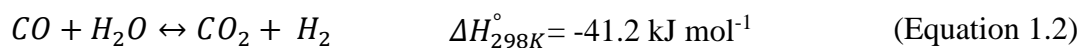
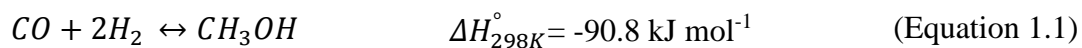


Figure 1.2 Major applications of methanol.

As a chemical feedstock, methanol are used in the production of formaldehyde and acetic acid (Huang and Tan, 2014; Ali *et al.*, 2015). For energy applications, methanol can be used directly to fuel automotive, ship and turbine engines (Kauw *et al.*, 2015; Methanol Institute, 2018). Besides, methanol has been actively investigated as hydrogen carrier in fuel cells (Li and Faghri, 2012; Baglio *et al.*, 2017). The synthesis of liquid methanol is considered as a route to store hydrogen energy more conveniently and safely (Olah *et al.*, 2006). Methanol is also consumed indirectly as transportation fuel via the production of dimethyl ether (DME) and biodiesel from transesterification (Methanol Institute, 2018).

In wastewater treatment plant, methanol is used in the denitrification process to convert nitrate to nitrogen gas which is then vented into atmosphere, thus preventing algal blooming in watersheds (Pan *et al.*, 2013). The methanol-to-olefins (MTO) process is a relatively new application of methanol that is rapidly growing now. Olefins (eg. ethylene, propylene) are commonly used in the production of plastic materials and are conventionally produced from steam cracking of hydrocarbons such as ethane and naptha (Honeywell UOP, 2018). This has limited the production of olefins to regions with access to ethane or naptha. The MTO technology provides a solution to overcome this limitation via the direct conversion of methanol to olefins, in which methanol can be produced from diverse resources such as coal and natural gas.

Currently, the industrial production of methanol is carried out almost exclusively using syngas (mixture of CO, CO₂ and H₂) derived from natural gas and coal over metal based catalyst, generally Cu/ZnO/Al₂O₃, at 5-10 MPa and 200-300°C via the following reactions (Wang *et al.*, 2011; Zangeneh *et al.*, 2011).

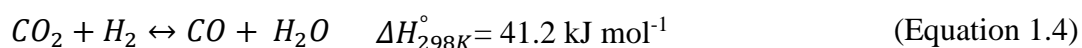


All the reactions described (Equation 1.1-1.3) are reversible. Thus, it is important to monitor the process conditions such as temperature, pressure and synthesis gas composition during operations. Generally, H₂:CO mole ratio of 2 and the ratio of (H₂+CO₂):(CO+CO₂) equal to or slightly above 2 in the synthesis gas are required in the production of methanol (Marine Methanol, 2017). As shown, the hydrogenation step to produce methanol could take place on both CO (Equation 1.1) and CO₂ (Equation 1.3). Additionally, CO and CO₂ are inter-convertible through the water-gas shift (WGS) reaction (Equation 1.2).

In November 2017, several methanol production plants in China were forced to shut down due to dwindling supply of natural gas as residential use was prioritized during the cold winter season (Liang, 2018). This has caused the regional methanol price to hover at high level. In Asia, the methanol price was recorded at USD 400/metric ton in November 2017 and the price was increased to USD 480/metric ton in February 2018 (Methanex, 2018). The short supply of methanol has also led to speculation that MTO plants may halt production or cut plant run rates because of the high methanol prices (Liang, 2018). The incident clearly reflects a pressing need to find a more sustainable alternative to produce methanol. In this regard, methanol production via direct CO₂ hydrogenation is a worthy option to reduce the dependency of methanol production on fossil-based resources.

1.2 Direct carbon dioxide (CO₂) hydrogenation to methanol

For long, the carbon source in industrial methanol synthesis has been subjected to debate until kinetic experiments and isotopic labeling studies, over Cu/ZnO catalyst, indicate that methanol formation is mainly from CO₂ and CO acts as source of CO₂ via WGS reaction (Liu *et al.*, 1985; Chinchén *et al.*, 1987). Following these findings, many research efforts are focused on the direct use of CO₂ in methanol synthesis. In direct CO₂ hydrogenation, the major reactions involved are methanol formation (Equation 1.1) and reverse water-gas shift reaction (RWGS) (Equation 1.4) (Razali *et al.*, 2012; Jadhav *et al.*, 2014).



Methanol production via direct CO₂ hydrogenation is a useful strategy to utilize CO₂ and a practical approach to sustainable development. The production of methanol by this alternative route and its use as fuels are the cores of the “methanol economy”, a notion proposed by Nobel Laureate Olah and co-workers (Olah *et al.*, 2006). In the “methanol economy” notion, CO₂ is captured from any natural or industrial sources, human activities or air by absorption. Then, the CO₂ is chemically transformed into methanol using hydrogen produced from water electrolysis.

Methanol production from direct CO₂ hydrogenation is advantageous as it reduces human dependency on fossil-based resources, thus, contributing to energy security and sustainable development. It also provides an alternative to CO₂ sequestration, a controversial CO₂ containment option which requires suitable sequestration sites and continuous monitoring of the CO₂ stored in the underground (Yuan *et al.*, 2016). Additionally, CO₂ sequestration increases the risk of exposure to

hazards in the events of leakage and earthquakes (Yuan *et al.*, 2016). Methanol production from direct CO₂ hydrogenation offers an attractive option to further extend industrialized CO₂ utilizations since the actual utilization now only represents a minor fraction of the anthropogenic emission (Aresta *et al.*, 2013). The alternative methanol synthesis route is predicted to deliver a carbon-neutral and unlimited source of energy, as well as convenient feedstock for producing other hydrocarbons (Olah *et al.*, 2006). Thus, it essentially substitutes petroleum oil and natural gas. This makes the lasting use of carbon-containing fuels possible and prevents excessive CO₂ emissions.

More recently, a new perspective on methanol synthesis from direct CO₂ hydrogenation has emerged, wherein the process is considered as a way to store surplus electrical energy produced from renewable energy sources (RES) such as wind, solar and hydraulic energy (Rivarolo *et al.*, 2016; González-Aparicio *et al.*, 2017). The integration of RES and methanol production from CO₂ hydrogenation is also known as power-to-methanol (PtMeOH) process. The success operation of methanol production from CO₂ hydrogenation at high efficiency using cheap electricity generated from RES can be expected to alleviate the threats of global warming and to fulfil the world demand for renewable energy (Atsonios *et al.*, 2016; Rivarolo *et al.*, 2016).

Despite considerable works have been conducted, the effectiveness of CO₂ utilization in the reaction remains unresolved. The inert property of CO₂ requires high performance catalyst and effective reaction conditions for its conversion into methanol (Ma *et al.*, 2009; Porosoff *et al.*, 2016). These barriers pose significant challenges and opportunities to researchers. Current achievements in catalytic CO₂ hydrogenation is still not satisfactory due to the lack of highly active catalyst to boost the efficiency of the reaction. In light of the above, more academia enthusiasm, industrial investment

and government supports are needed to further advance understanding on rational catalyst design for CO₂ hydrogenation to methanol.

1.3 Problem statement

Although direct CO₂ hydrogenation to methanol has been the subject of many CO₂ utilization studies over the past few decades, continuous research is still required for the decentralization of the technology and developing catalysts (new or reformulation) remains as a useful approach in resolving the present limitations.

An immediate challenge in the reaction of direct CO₂ hydrogenation to methanol is the presence of the competing RWGS reaction. At high reaction temperature ($\geq 220^{\circ}\text{C}$), most of the CO₂ are converted to CO through RWGS and/or methanol decomposition (Arena *et al.*, 2013; Xiao *et al.*, 2015). Hence, the methanol selectivity and yield are severely lowered at high reaction temperature. Thermodynamically, the RWGS can be suppressed by employing low reaction temperature ($\leq 200^{\circ}\text{C}$) (Saeidi *et al.*, 2014). Yet, the conversion of CO₂ to methanol at low reaction temperature is usually low and therefore limits the methanol yield. Therefore, a rational catalyst design for direct CO₂ hydrogenation to methanol should promote CO₂ conversion at low reaction temperature and stabilize the reaction intermediates to form methanol. Herein, multi-component copper-based catalyst supported on pre-shaped porous silica is proposed and developed for direct CO₂ hydrogenation to methanol.

In current study, copper (Cu) has been selected as the main active metal for investigation since it is widely proven active for methanol synthesis via direct CO₂ hydrogenation and it has been extensively discussed in many review articles (Jadhav *et al.*, 2014; Ali *et al.*, 2015; Li *et al.*, 2015). Furthermore, copper is the only metal

element identified to exhibit the ability to catalyse CO₂ hydrogenation to methanol on industrial scale (Li *et al.*, 2015). The performance of copper-based catalysts is frequently correlated to large copper surface area, high copper dispersion, and synergistic interactions between copper and oxide support (Natesakhawat *et al.*, 2012; Zhang *et al.*, 2012; Bonura *et al.*, 2014). These observations accentuated the opportunities to enhance catalyst performance by manipulating the properties of copper in the catalyst.

The investigations on multi-component copper-based catalysts have been documented since decades ago and a resurgence in the topic has been observed in recent years due to our improved understanding on multi-functionality of mixed metal-oxide(s) (Yang *et al.*, 2012; Rodriguez *et al.*, 2015). A multi-component catalyst generally consists of several metals, each may have different catalytic properties and hence allows the potential formation of adsorption/reaction sites with different nature (Okumura *et al.*, 2003; Graciani *et al.*, 2014). This points to the prospects to enhance methanol production from direct CO₂ hydrogenation through an appropriate combination of components that benefit the reaction.

As mentioned earlier, the performance of copper-based catalysts is highly dependent on the properties of copper. It could be conceivably hypothesized that pre-shaped porous supports can have significant effect on the formation and growth of copper crystallites and thereby affect the performance of the catalyst. This is supported by the findings of several research groups (Koizumi *et al.*, 2009; Prieto *et al.*, 2013; Osakoo *et al.*, 2014). Their studies have shown the effect of porous supports in modifying the properties of active metal sites, thus, affecting the performance of catalysts. However, none of these studies are intended for examining the effect of porous supports on copper crystallites in the reaction of direct CO₂ hydrogenation to

methanol. The study by Koizumi et al. (2009) has been focused on palladium-based catalysts for direct CO₂ hydrogenation while Osakoo et al. (2014) focused on cobalt-catalysts for Fischer-Tropsch reaction. Meanwhile, the study by Prieto et al. (2013) on copper-based catalysts has been conducted using syngas as reactants for methanol production. In view of these, the effect of porous supports on the formation and growth of copper crystallites in the reaction of direct CO₂ hydrogenation is worth of investigation.

Over porous catalysts, the reaction of direct CO₂ hydrogenation to methanol can be viewed as to proceed at the exterior and interior surfaces of the catalysts. The process is accompanied by pore diffusion of reactants and reaction products into and out of catalyst grains. The rate of reactant conversion and product formation in a gas-solid heterogeneous catalytic reaction is principally relied on the diffusion or mass transfer between gas and solid phase (Satterfield, 1991; Fogler, 2006). Although investigation on effective diffusivity (catalyst pore-geometry dependent coefficient) of molecules in porous catalysts has theoretical and practical importance, the subject has not been adequately addressed in literature.

To address the gaps of knowledge above, a multi-component copper-based catalyst supported on pre-shaped porous silica is developed for direct CO₂ hydrogenation to methanol. The functionality of the catalyst components and the descriptors that influence the performance of the catalyst are determined. Then, the morphological impact of porous supports on the formation and growth of copper crystallites and the effective diffusivity of CO₂ molecules in the catalyst are investigated.

1.4 Research objectives

The present study has the following objectives: -

1. To develop multi-component copper-based catalyst for direct CO₂ hydrogenation to methanol
2. To investigate the morphological impact of siliceous porous supports on copper crystallites and effective diffusivity of catalyst
3. To study the effect of process conditions on the performance of catalyst in the reaction
4. To assess the stability of the multi-component copper-based catalyst

1.5 Scope of study

In its broadest sense, the direct conversion of CO₂ to methanol requires a large scale of study and therefore it would be impossible for such task to be undertaken in a single research work. Thus, the present study is limited to heterogenous catalyst design, i.e. to develop multi-component copper-based catalyst supported on pre-shaped porous silica.

The performance of the synthesized catalyst is tested via thermochemical conversion route. Thermochemical conversion route is chosen over electrochemical and photochemical conversion routes because it is the most promising and mature route for methanol production from direct CO₂ hydrogenation. All the catalysts are synthesized using citric acid impregnation method because the method has been reported to preserve the structure of pre-shaped siliceous porous support and it promotes homogenous distribution of active components (Van Dillen *et al.*, 2003; Calderon-Magdaleno *et al.*, 2014).

In the screening of Cu:Zn mole ratio, the loading of Cu is varied from 0.15-1.05 mole (at the interval of 0.15 mole) while the loadings of Zn and SBA-15 are fixed at 0.15 mole and 1.0 mole, respectively. Then, the most active catalyst is investigated for the introduction of third metallic component (as promoter). The screening of promoter is limited to transition metal (Cr, Mn, Fe, Co, Ni). The selection is based on the findings of computational studies which have revealed the effect of transition metal on modifying the copper surface properties and the performance of catalysts in CO₂ reduction to methanol and CO (Liu *et al.*, 2012; Yang *et al.*, 2012).

The investigation on the morphological impact of porous supports on copper crystallites and effective diffusivity of catalysts is achieved by varying the types of siliceous porous supports in the catalyst. Meanwhile, the preparation method and composition of the catalysts are held constant. The porous supports selected for investigations are SBA-15, MCF and KIT-6. These materials are selected because they have distinctive morphology and with high reproducibility during synthesis. More importantly, they are all silica-based porous materials and therefore comparable. The formation and growth of copper crystallites in the catalysts are examined. The effective diffusivities of the synthesized catalysts are also examined by assuming molecular pore diffusion occurs in the transition region, whereby both Knudsen ($D_{K,eff}$) and bulk diffusion ($D_{12,eff}$) are important.

After identifying the most active catalyst from the above, a more in-depth study on the performance of the catalyst is conducted. The effects of process conditions on the performance of the catalyst in direct CO₂ hydrogenation to methanol are investigated. The process parameters chosen to be investigated are weight-hourly space velocity (WHSV, 8-120 L/g_{cat}.h), reaction temperature (160-260°C) and reaction pressure (1.0-5.0 MPa). The range of process parameters are selected by considering

relevant literature and equipment limitations. The apparent activation energies of methanol and CO formation are also evaluated. Finally, the stability of the catalyst in 120 h time-on-stream is assessed.

1.6 Thesis organization

This thesis consists of five chapters. Chapter One (Introduction) includes a brief introduction on the importance of methanol as a global commodity and the current industrial practice to produce it. Then, the potential of producing methanol from direct CO₂ hydrogenation is discussed. Problem statement is defined after reviewing the existing limitations in direct CO₂ hydrogenation to methanol. A rational catalyst design for direct CO₂ hydrogenation to methanol is proposed to overcome the current limitations. The objectives of the present work are carefully set and the scope of study is given in this chapter.

Chapter Two (Literature Review) summarizes the theoretical background, contemporary knowledge and important findings on direct CO₂ hydrogenation to methanol. The chapter starts with an overview of conversion routes for CO₂ hydrogenation and justify the current selection to explore thermochemical conversion route. Then, the thermodynamic analysis of the reaction is presented followed by a discussion on the reaction mechanisms and CO₂ activation. Next, the heterogenous catalysts developed in past studies and the steps in a catalytic reaction are reviewed. A summary is provided at the end of the chapter.

Chapter Three (Materials and Methods) describes the experimental setup and catalyst synthesis procedures of the present work. Information of all the materials and chemicals used are listed. The characterization techniques used to examine the synthesized catalysts and the details on the equipment settings are provided.

Chapter Four (Results and Discussions) presents the results and the discussion of current research. Characterizations and catalytic performance of all the synthesized catalysts are presented in this chapter. The catalyst performances are correlated in a fundamental fashion to the properties of catalysts. The effects of process conditions (WHSV, temperature and pressure) on the reaction and the apparent activation energies (E_a) for methanol and CO formation are discussed. The stability of the most active catalyst in 120 h time-on-stream is presented at the end of the chapter.

Chapter Five (Conclusions and Recommendations) summarizes the results of the present research and the recommendations for future study. The chapter includes the overall research findings and the concluding remarks. Lastly, recommendations for future study are proposed. These recommendations are given based on the limitations of the present work and the difficulties encountered.

CHAPTER TWO

LITERATURE REVIEW

This chapter is a review on the theoretical background and contemporary findings on direct CO₂ hydrogenation to methanol. Section 2.1 presents the available conversion routes and justifies current selection in investigating thermochemical conversion. The thermodynamic analysis and the reaction mechanisms are discussed in Section 2.2 and 2.3, respectively. Insights on CO₂ activation are in Section 2.4. Previous researches on heterogeneous catalysts for CO₂ hydrogenation to methanol are collected in Section 2.5. The steps in a catalytic reaction are discussed in Section 2.6. Finally, the chapter ends with a summary of literature review, Section 2.7.

2.1 Conversion routes for direct CO₂ hydrogenation to methanol

In conjunction with the introduction of CO₂ utilization concept, researchers have been actively exploring and developing routes for direct CO₂ hydrogenation to methanol. The conversion routes explored currently can be briefly categorized according to the forms of external energy use to drive the reaction. The external energy supplied could be in the forms of heat, electrons and irradiation, which correspond to thermochemical, electrochemical and photochemical conversion (Alper and Orhan, 2017).

Electrochemical and photochemical conversions are sometimes regarded as the more “intelligent” routes for CO₂ utilization (Alper and Orhan, 2017). The perspective could be due to the analogies of these conversion routes to natural photosynthesis and the inherent difficulties in operating thermochemical plant while minimizing CO₂ emission in the process. For instance, the heating and high-pressure conditions in

thermochemical conversion are energy-intensive. Clearly, the electricity needed to power the thermochemical plant must be from non-fossil sources (e.g. geothermal, wind, hydroelectric) in order to limit CO₂ emission. In stark contrast, electrochemical and photochemical conversions are known to function at mild or even ambient conditions. Furthermore, the hydrogen consumed in thermochemical CO₂ hydrogenation should also be produced from non-fossil fueled technology. In fact, hydrogen production has been considered as a major cost in methanol production via thermochemical CO₂ hydrogenation (Jadhav *et al.*, 2014; Rivera-tinoco *et al.*, 2016). In this regard, the hydrogen in electrochemical and photochemical CO₂ conversion could be supplied by the parallel water splitting reaction.

Although conceptually attracting, there are many constraints related to electrochemical and photochemical conversions that are yet to be overcome. Most importantly, the efficiencies of these conversion routes are still far behind their practical applications. Both electrochemical and photochemical conversions involve multi-electron and multi-proton transfer. Referring to Equation 2.1, the methanol synthesis reaction via electrochemical or photochemical CO₂ hydrogenation involve six electrons and six protons transfer (Centi and Perathoner, 2009). Therefore, high transfer efficiency is a prerequisite for these conversion routes to function at optimum.



In electrochemical conversion, CO₂ reduction is competed by hydrogen evolution as side product when the reaction is conducted in aqueous electrolyte or solvent containing O-H and/or N-H bonds (Alper and Orhan, 2017). Additionally, the low solubility of CO₂ in aqueous electrolyte at standard temperature and pressure resulted in small amount of CO₂ available for reaction (Centi and Perathoner, 2009). Finding

electrodes with high stability is also a main challenge in realizing efficient electrochemical conversion of CO₂ (Olajire, 2013). The electricity required in electrochemical conversion also must come from non-fossil sources. In photochemical conversion, the discovery of non-noble metal photocatalysts that maximize light utilization, hinder electron-hole recombination, and facilitate charge separation and migration are still scientific hurdles that require sensible solutions (Alvarez *et al.*, 2017). Also, the methanol selectivity in photochemical conversion is impeded by hydrogen evolution reaction. Moreover, innovation and improvement in photoreactor design to harness the full potential of solar energy are still lacking.

By far, thermochemical conversion is still the most promising and mature route for direct CO₂ hydrogenation to methanol. This is proven by the successful operation of such chemical plants at commercial-scale. Considering this, Carbon Recycling International (CRI) in Iceland is the major player in the industry. Since 2011, CRI has been operating thermochemical plant to catalytically convert CO₂ in flue gas to methanol. The flue gas is captured from a geothermal power plant which also supplies electricity to the plant. In 2015, CRI has expanded the plant capacity from 1.3 million liters methanol per year to more than 5 million liters methanol per year (Carbon Recycling International, 2016). Annually, the plant recycles 5.5 thousand tonnes of CO₂ which otherwise would be released into the atmosphere. It is worth mentioning that the hydrogen consumed in the reaction are sourced from water splitting powered by renewable electricity, thus making the whole methanol production process a model demonstration of clean technology. Thermochemical conversion of CO₂ to methanol is also explored by Mitsui Chemicals in Japan. A pilot plant has been launched in Osaka Works since 2009 and many verification tests have been conducted. Currently, they are working towards commercialization of the process (Mitsui Chemicals, 2016).

The enthusiasms shown by these renown conglomerates indicate that the aforesaid drawbacks of thermochemical CO₂ conversion could be overcome by careful selection of plant locations which shall ease access to renewable electricity.

As presented, electrochemical and photochemical are attractive options in converting CO₂ to methanol. However, these conversion routes are yet ready for commercial-scale deployment and more research breakthroughs are needed. Thus, it can be expected that thermochemical conversion of CO₂ to methanol will continue to dominate the near future researches for CO₂ utilization. Improving the efficiency of the reaction is crucial for encouraging the decentralize of the technology and this is achievable via the discovery of active catalysts with high selectivity and stability. An active and highly selective catalyst will reduce the costs for reactant recycling and methanol purification. High stability of the catalyst is desirable as it aids to reduce the cost for their replacement. In view of these, current research is focus on catalyst development for thermochemical CO₂ conversion to methanol. More in-depth discussion on the technical aspects is presented in the following sections.

2.2 Thermodynamic analysis

The conversion of CO₂ to methanol is highly desirable since it is a promising approach to reduce human dependence on fossil fuel and to reduce atmospheric CO₂ actively. In order to control the reaction pathway of CO₂ conversion by hydrogenation, it is indispensable to understand the thermodynamics of the reaction of interest and the side reaction involved. In CO₂ hydrogenation to methanol, reverse water-gas shift (RWGS) often occurs as the major side reaction that leads to excessive consumption of hydrogen to produce unwanted CO and water. The enthalpy and Gibbs free energy

changes of methanol synthesis via CO₂ hydrogenation and RWGS are summarized in Table 2.1.

Table 2.1 Enthalpy and Gibbs free energy change of methanol synthesis via CO₂ hydrogenation and RWGS (Centi & Perathoner, 2009; Akarmazyan, 2015).

Reaction description	Reaction formula	ΔH_{298K}° (kJ/mol)	ΔG_{298K}° (kJ/mol)
Methanol synthesis via CO ₂ hydrogenation	$CO_2 + 3H_2 \leftrightarrow CH_3OH + H_2O$	-49.5	3.72
RWGS	$CO_2 + H_2 \leftrightarrow CO + H_2O$	41.2	28.6

Methanol synthesis is an exothermic reaction with positive Gibbs free energy change at 298K. Considering the Gibbs-Helmholtz relationship, Equation 2.2, the Gibbs free energy change increases with increasing reaction temperature, thus, increasing temperature is not favourable for the reaction.

$$\Delta G^{\circ} = \Delta H^{\circ} - T\Delta S^{\circ} \quad \text{Equation 2.2}$$

The reaction is also accompanied by the reduction of the number of molecules from 4 to 2 molecules. Thermodynamically, low temperature and high-pressure reaction conditions are favourable for methanol synthesis. For example, at CO₂:H₂ feed ratio of 1:3, the equilibrium yield of methanol at 200°C and 5 MPa is approximately 27%. At the same feed ratio, when the reaction conditions are changed to 240°C and 3 MPa, the equilibrium yield of methanol drops to approximately 8% (Arena *et al.*, 2013).

Although low reaction temperature ($\leq 200^{\circ}\text{C}$) in methanol synthesis is highly desirable from thermodynamic and economic perspectives, the reaction is kinetically limited as a substantial amount of external energy is required to activate CO₂ molecules. CO₂ conversion at low reaction temperature is usually too low for practical

operation. Instead, reaction temperatures of $\geq 220^{\circ}\text{C}$ are commonly reported to be the optimum to achieve reasonable CO_2 conversion, regardless the type of catalyst and reaction pressure (Liu *et al.*, 2013; Porosoff *et al.*, 2014; Saeidi *et al.*, 2014).

The approach to facilitate CO_2 conversion by increasing reaction temperature inevitably enhances RWGS, which is an endothermal reaction with positive Gibbs free energy change at 298K. The Gibbs free energy change decreases with increasing reaction temperature. Hence, the increases of reaction temperature could enhance RWGS. As expected, the formation of unwanted CO in RWGS reduces methanol selectivity and yield. For instance, the methanol selectivity and yield obtained over Cu-ZnO-TiO₂ catalyst at 220°C were approximately 50% and 7.5%, respectively. As the reaction temperature increased to 260°C , the methanol selectivity and yield decreased to approximately 33% and 6.3%, respectively (Xiao *et al.*, 2015).

Considering the above, it is difficult to drive the methanol synthesis reaction to equilibrium by employing low reaction temperature alone. The CO_2 conversion and methanol yield achieved experimentally are usually lower compared to the equilibrium due to the kinetic limitation. In the study by Bansode and Urakawa (2014), high reaction pressure approach has been proposed to enhance methanol productivity via direct CO_2 hydrogenation. The approach has been claimed to shift equilibrium conversion, forming unique phase and states of reaction mixture and catalysts which boost the catalytic activity. At $\text{CO}_2\text{:H}_2$ feed ratio of 1:3, reaction temperature 260°C and pressure as high as 36 MPa, the methanol yield was 26.6%. Although outstanding yield has been achieved in the study, the pressure applied was too high for economic conversion (Porosoff *et al.*, 2016). Such high-pressure process would raise long-term safety concerns and expensive precaution measures are often required.

Since methanol production via CO₂ hydrogenation is thermodynamically limited at high temperature, it is more promising to explore the reaction at low temperature, in which the kinetic limitation ensued can be alleviated through the development of active catalyst. In order to minimize the reconstruction of existing methanol synthesis facilities, the active catalyst should be functional under moderate reaction pressure of not more than 5 MPa.

2.3 Reaction mechanisms

Unraveling the underlying mechanisms of CO₂ hydrogenation to methanol is a fundamental step in identifying descriptors that are valuable in developing superior catalyst. The identification of reaction mechanism is more conveniently achieved by theoretical calculations rather than experimental techniques due to the difficulties to measure transient intermediate species. Extensive efforts have been devoted to establishing the reaction mechanism of CO₂ hydrogenation to methanol in the past few decades. Though controversies remain, studies on copper-based model catalyst highlighted the viability of formate pathway, RWGS + CO-hydrogenation pathway and hydrocarboxyl pathway in CO₂ hydrogenation to methanol. The reaction mechanism networks are summarized in Figure 2.1.

CO₂ hydrogenation to methanol has long being assumed to progress via the formate pathway. This is supported by the observation of almost a full monolayer of formate (HCOO*) on Cu surface in X-ray photoelectron spectroscopy (XPS) and temperature-programmed desorption (TPD) experiments (Yoshihara and Campbell, 1996). In the formate pathway, CO₂ hydrogenation leads to the formation of formate (HCOO*), followed by dioxomethylene (H₂COO*), formaldehyde (H₂CO*) and methoxy (H₃CO*). The hydrogenation of HCOO* and H₂COO* intermediates are

widely claimed to be the rate-limiting steps (Fujitani *et al.*, 1997; Yang *et al.*, 2010). Furthermore, H_2COO^* has been found unstable and could be decomposed to HCOO^* through the reverse reaction (Hu *et al.*, 1999).

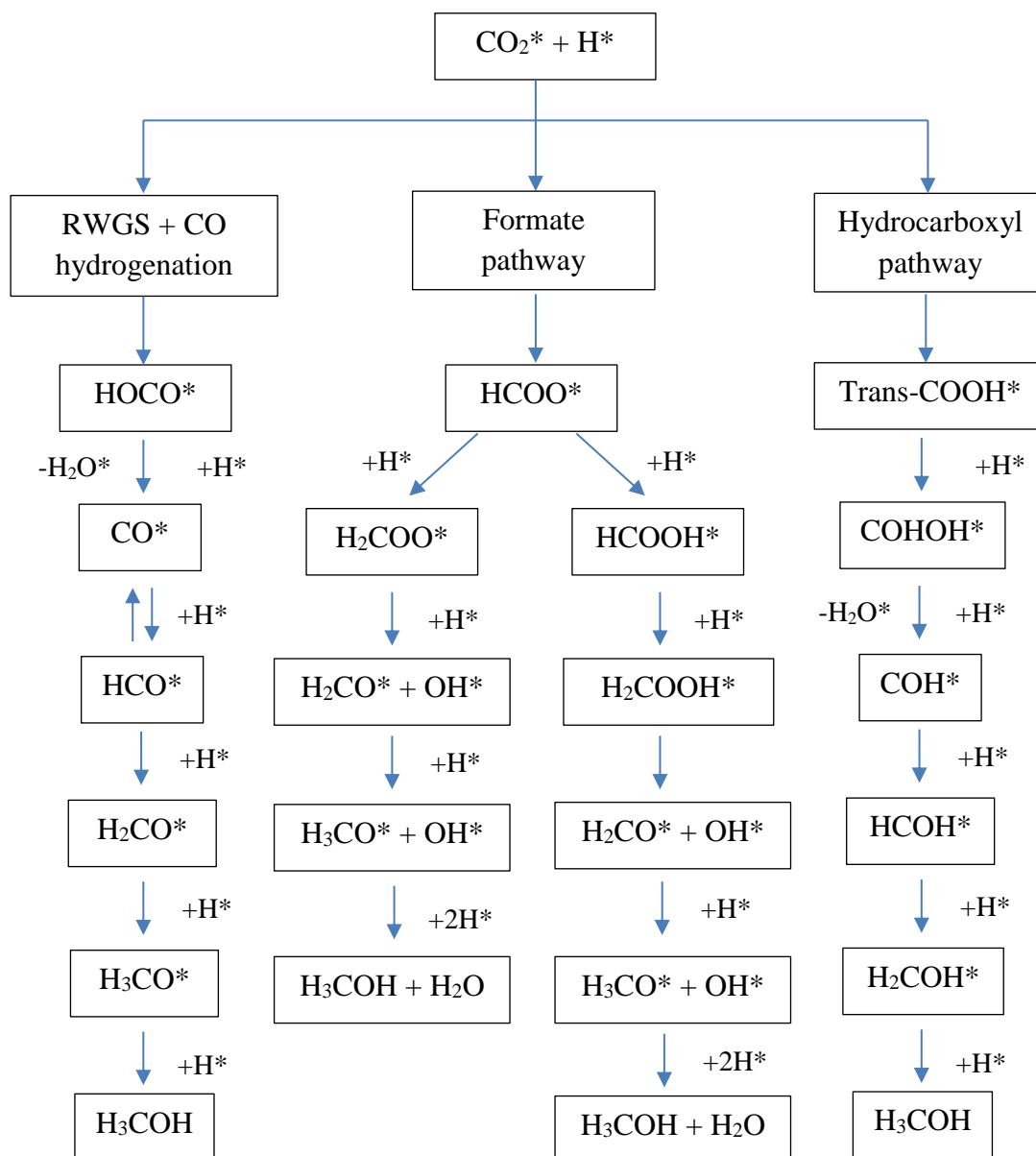


Figure 2.1 Reaction mechanism networks of CO_2 hydrogenation to methanol (Grabow and Mavrikakis, 2011; Zhao *et al.*, 2011; Tao *et al.*, 2013; Yang *et al.*, 2013).

More recently, Grabow and Mavrikakis (2011) has proposed the formation of formic acid (HCOOH^*), rather than H_2COO^* , from subsequent hydrogenation of HCOO^* . This finding can be viewed as a revision of the formate pathway. The

formation of HCOOH^* ($\Delta E = 0.23$ eV) has been found far less endothermic than H_2COO^* ($\Delta E = 0.87$ eV). More importantly, the comparison of the reaction coordinates shows that the activation barriers for HCOO^* hydrogenation to HCOOH^* (0.91 eV) was lower than HCOO^* hydrogenation to H_2COO^* (1.59 eV) by 0.68 eV. A similar revised formate pathway has also been reported by Behrens *et al.* (2012).

In the RWGS + CO-hydrogenation pathway, CO_2 is converted to CO and subsequently hydrogenated to methanol via intermediate formyl (HCO^*) and H_2CO^* . The rate-limiting step in RWGS + CO-hydrogenation pathway is the hydrogenation of CO^* and HCO^* intermediates. The CO^* could desorb from catalyst surface and HCO^* preferentially decompose back to CO and H through the reverse reaction (Zhao *et al.*, 2011; Yang *et al.*, 2012). These constraining factors explain the observation of CO formation as the major by-product and low methanol yield in experimental studies. Using a combination of density functional theory (DFT) calculations, kinetic Monte Carlo (KMC) simulations, *in-situ* diffuse reflectance infrared Fourier transform spectroscopy (DRIFTS) measurements and steady-state flow reactor tests, Kattel *et al.* (2016) has shown that methanol synthesis from CO_2 hydrogenation on Cu surface proceeds mainly via RWGS + CO-hydrogenation pathway while the contribution from formate pathway is limited over time due to the high stability of $^*\text{HCOO}$ on the surface, causing the poisoning of active sites. Therefore, $^*\text{HCOO}$ acts as spectator species eventually.

In hydrocarboxyl pathway, CO_2 hydrogenation to hydrocarboxyl (trans- COOH) is thought to be kinetically favorable than formate hydrogenation due to a unique hydrogen transfer mechanism in the presence of water (Zhao *et al.*, 2011). The presence of water promotes the formation of COOH^* , which is the rate-limiting step in the hydrocarboxyl mechanism. In the unique hydrogen transfer mechanism, weakly

bonded CO₂ is hydrogenated by one of the hydrogen atoms in water as surface hydrogen begins to strongly interact with the water molecule. The trans-COOH is then converted to dihydroxycarbene (COHOH*), followed by hydroxymethylidyne (COH*) and three consecutive hydrogenation steps to form hydroxymethylene (HCOH*), hydroxymethyl (H₂COH*) and methanol (Zhao *et al.*, 2011). This pathway redefines the role of water which has been conventionally viewed as inhibitor that deactivates catalyst by enhancing copper sintering (Arena *et al.*, 2009; Samei *et al.*, 2012). The investigation by Yang *et al.* (2013) has concluded the importance of the presence of water, produced from methanol synthesis and RWGS, to serve as an auto-catalyst to initiate both reactions. In the absence of water, methanol cannot be produced via CO₂ hydrogenation.

The proposed reaction mechanisms provide invaluable perspectives on rational catalyst design for direct CO₂ hydrogenation to methanol. Based on the discussed mechanisms, an ideal catalyst should be able to lower the energy barriers of stepwise intermediates-hydrogenation. The catalyst should stabilize intermediates, thus preventing their dissociation due to the reverse reactions. In addition, the presence of abundant of atomically activated H* species is important for enhancing stepwise-hydrogenation. Therefore, the ideal catalyst should possess strong hydrogenation strength to dissociate hydrogen. While experiments provide the evidence of water as auto-catalyst to initiate methanol synthesis reaction, water also has detrimental effects on the stability of copper nanoparticles in catalysts. Hence, enhancement of catalyst hydrophobicity is a useful strategy to abate catalyst deactivation due to copper crystallite growth. Besides, immobilization of copper nanoparticles in catalysts by inducing strong metal-support interaction could also prevent copper sintering through migration-coalescence during reaction.

2.4 Activation of CO₂ molecules

CO₂ molecule is thermodynamically stable due to its negative electron affinity (-0.6 eV) and large ionization potential (13.73 eV) (Viswanathan, 2013). The Gibbs energy of formation (ΔG_{298K}°) of the molecule has a large negative value of -394.6 kJ/mol (Havran *et al.*, 2011). Consequently, CO₂ conversion is energetically difficult under mild conditions. Often, a large input of energy, high pressure condition, the presence of active reductant and catalyst are required for the conversion of CO₂ (Toda *et al.*, 2013).

The bending of CO₂ molecule from its linear geometry is commonly accepted as one of the essential steps in CO₂ activation (Zangeneh *et al.*, 2011; Ge, 2013; Alvarez *et al.*, 2017). In heterogenous catalysis, the coordination of CO₂ molecule to a catalytically active metal site could occur via four modes, i.e. (a) donating oxygen lone pair electron to a strong Lewis acid site, (b) accepting electrons through its carbon atom in one of the C-O bond to form unidentate, (c) complexing with C=O double bond to form bidentate and (d) ionic bonding to form metal carboxylate, M⁺CO₂⁻ (often encountered in CO₂ adsorption to alkali or alkaline-earth metals) (Liu *et al.*, 2013; Ge, 2013). These coordination modes are illustrated in Figure 2.2.

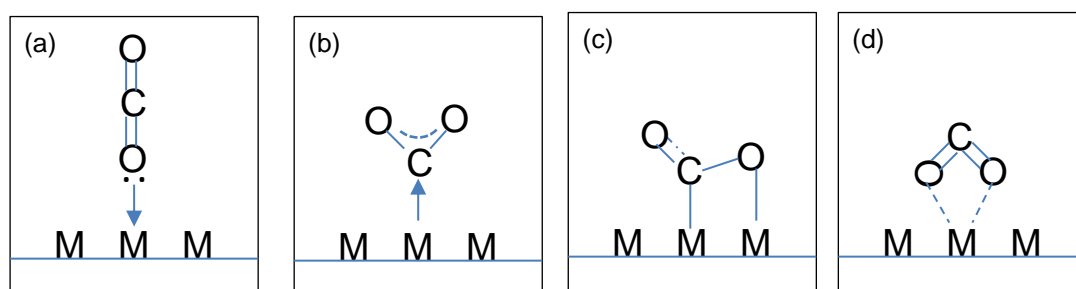


Figure 2.2 Coordination modes of CO₂ molecule to active metal site (Ge, 2013; Liu *et al.*, 2013).